

# Antibody therapy targeting the CD47 protein is effective in a model of aggressive metastatic leiomyosarcoma

Badreddin Edris<sup>a,b</sup>, Kipp Weiskopf<sup>c</sup>, Anne K. Volkmer<sup>c</sup>, Jens-Peter Volkmer<sup>c</sup>, Stephen B. Willingham<sup>c</sup>, Humberto Contreras-Trujillo<sup>c</sup>, Jie Liu<sup>c</sup>, Ravindra Majeti<sup>c</sup>, Robert B. West<sup>a</sup>, Jonathan A. Fletcher<sup>d</sup>, Andrew H. Beck<sup>e</sup>, Irving L. Weissman<sup>a,c,1,2</sup>, and Matt van de Rijn<sup>a,1,2</sup>

<sup>a</sup>Department of Pathology, and <sup>b</sup>Department of Genetics, Stanford University Medical Center, Stanford, CA 94305; <sup>c</sup>Institute for Stem Cell Biology and Regenerative Medicine and the Ludwig Cancer Institute, Stanford University School of Medicine, Stanford, CA 94305; <sup>d</sup>Department of Pathology, Brigham and Women's Hospital, Boston, MA 02115; and <sup>e</sup>Department of Pathology, Beth Israel Deaconess Medical Center, Boston, MA 02115

Contributed by Irving L. Weissman, January 3, 2012 (sent for review December 13, 2011)

**Antibodies against CD47, which block tumor cell CD47 interactions with macrophage signal regulatory protein- $\alpha$ , have been shown to decrease tumor size in hematological and epithelial tumor models by interfering with the protection from phagocytosis by macrophages that intact CD47 bestows upon tumor cells. Leiomyosarcoma (LMS) is a tumor of smooth muscle that can express varying levels of colony-stimulating factor-1 (CSF1), the expression of which correlates with the numbers of tumor-associated macrophages (TAMs) that are found in these tumors. We have previously shown that the presence of TAMs in LMS is associated with poor clinical outcome and the overall effect of TAMs in LMS therefore appears to be protumorigenic. However, the use of inhibitory antibodies against CD47 offers an opportunity to turn TAMs against LMS cells by allowing the phagocytic behavior of resident macrophages to predominate. Here we show that interference with CD47 increases phagocytosis of two human LMS cell lines, LMS04 and LMS05, *in vitro*. In addition, treatment of mice bearing subcutaneous LMS04 and LMS05 tumors with a novel, humanized anti-CD47 antibody resulted in significant reductions in tumor size. Mice bearing LMS04 tumors develop large numbers of lymph node and lung metastases. In a unique model for neoadjuvant treatment, mice were treated with anti-CD47 antibody starting 1 wk before resection of established primary tumors and subsequently showed a striking decrease in the size and number of metastases. These data suggest that treatment with anti-CD47 antibodies not only reduces primary tumor size but can also be used to inhibit the development of, or to eliminate, metastatic disease.**

**L**eiomyosarcoma (LMS) is a neoplasm of smooth muscle cells that can arise in the uterus or in soft tissue throughout the body. Currently, there exist limited therapeutic options for patients diagnosed with LMS, and the lack of actionable prognostic markers and a limited understanding of the biological mechanisms underlying LMS complicate the clinical management of these tumors (1). The rate of metastatic relapse for these tumors following local treatment is ~40% at 5 y, leading to, in most cases, an incurable condition (2, 3).

Macrophages are monocyte-derived phagocytic cells that play crucial roles in adaptive and innate immunity. Tumor-associated macrophages (TAMs) also play important roles in tumor behavior, depending on their polarization. M1, or "classically activated" TAMs, can mediate anticancer effects by eliciting antitumor-adaptive immunity mechanisms that include phagocytosis. In contrast, M2, or "alternatively activated" TAMs, suppress adaptive immunity and promote a tumor microenvironment (TME) that can augment cancer progression. In many types of carcinomas, TAMs function as promoters of cancer progression, presumably via their ability to mediate tumor angiogenesis, increase extracellular matrix breakdown, aid in tumor invasion, and augment the capacity of tumor cells to form distant metastases (4–6). The TME's role as a non-neoplastic component of tumors has been studied extensively in carcinomas but remains less well characterized in sarcomas. Consistent with the findings in carcinomas, we have previously shown

that in LMS, a high density of TAMs predicts poor patient outcome, and that these TAMs are likely attracted to the primary tumor site by secretion of the macrophage chemoattractant colony-stimulating factor-1 (CSF1) by tumor cells (7, 8). Moreover, in extrauterine LMS, we showed a correlation between CSF1 expression and a highly vascularized TME, consistent with the protumorigenic effects of TAMs (9). Therefore, CSF1 secretion by LMS tumor cells leads to an increase in TAMs and results in poor clinical outcome, indicating that in LMS, TAMs likely behave according to the M2 phenotype and that inhibition of CSF1 may form a novel therapeutic approach in LMS, both by inhibiting M2 polarization and by decreasing TAM accumulation in the TME, as has been shown previously in a mouse model of osteosarcoma (10). In the present work, we explore the feasibility of an alternative and possible complementary approach to treat LMS, which allows macrophages to exert their M1 phenotype by removing inhibitory factors for phagocytosis.

CD47 is a widely expressed transmembrane protein that serves as a ligand to signal regulatory protein- $\alpha$  (SIRP $\alpha$ ), a molecule expressed on macrophages (11). The interaction between CD47 and SIRP $\alpha$  results in the inhibition of phagocytosis through a signaling cascade transmitted via phosphorylation of the immunoreceptor tyrosine-based inhibition motif present on the cytoplasmic tail of SIRP $\alpha$  (12). Previous work in experimental models of bladder cancer, leukemia, and lymphoma has demonstrated that inhibiting the interaction between CD47 and SIRP $\alpha$  using anti-CD47 monoclonal antibodies (mAbs) allows for increased phagocytosis of cancer cells by macrophages *in vitro* and a decrease in tumor burden *in vivo* (13–17).

Given the prognostic significance of TAM infiltration in LMS, as well as the potential for anti-CD47 mAbs to decrease tumor burden in experimental models of cancer, we sought to test the feasibility of targeted CD47 therapeutically in LMS. Here, we demonstrate that CD47 is present on LMS tumor cells at higher levels than in benign leiomyomas and that anti-CD47 mAbs enable phagocytosis of two human LMS cell lines by macrophages *in vitro*. Furthermore, we show that treatment with a novel, fully humanized anti-CD47 mAb inhibits primary tumor growth in two xenotransplantation models of LMS, uniquely demonstrating the potential efficacy of anti-CD47 treatment in soft-tissue sarcoma. We also describe the development of a metastatic xenotransplantation model of LMS, whereby, similar to what is observed in human patients, mice develop

Author contributions: B.E., K.W., J.-P.V., S.B.W., I.L.W., and M.v.d.R. designed research; B.E., K.W., A.K.V., J.-P.V., S.B.W., and H.C.-T. performed research; J.L., R.M., and J.A.F. contributed new reagents/analytic tools; B.E., K.W., J.-P.V., S.B.W., R.B.W., A.H.B., I.L.W., and M.v.d.R. analyzed data; and B.E., I.L.W., and M.v.d.R. wrote the paper.

The authors declare no conflict of interest.

Freely available online through the PNAS open access option.

<sup>1</sup>I.L.W. and M.v.d.R. contributed equally to this work.

<sup>2</sup>To whom correspondence may be addressed. E-mail: irv@stanford.edu or mrijn@stanford.edu.

This article contains supporting information online at [www.pnas.org/lookup/suppl/doi:10.1073/pnas.1121629109/-DCSupplemental](http://www.pnas.org/lookup/suppl/doi:10.1073/pnas.1121629109/-DCSupplemental).

metastases after resection of their primary tumors. In this model, we show that anti-CD47 mAb treatment can diminish the size and incidence of secondary tumors, and dramatically inhibits the presence of lung metastases. Taken together, these results demonstrate that anti-CD47 mAb therapy may be a promising treatment for LMS and that targeting CD47 on LMS cells has the potential to change the behavior of resident TAMs to inhibit, rather than promote, tumor growth.

## Results

**CD47 Is Expressed at Higher Levels on LMS Compared with Benign Leiomyoma and Normal Muscle.** We evaluated the level of expression of mRNA for *CD47* and TAM markers *CD68* and *CD163* in a group of 51 cases of LMS and 19 benign leiomyomas. *CD47*, *CD68*, and *CD163* expression were all significantly up-regulated on LMS cases versus benign leiomyoma cases (Fig. 1A). We next analyzed CD47 protein expression on 16 LMS, three leiomyoma, and three normal muscle samples using frozen section immunohistochemistry. Consistent with our gene-expression profiling results, CD47 expression was high on 14 of the 16 LMS samples, but low or absent on five of the six leiomyoma and normal muscle samples (Fig. 1B, Fig. S1, and Table S1).

**Anti-CD47 Antibodies Enable Phagocytosis.** In experimental models of leukemia, lymphoma, and bladder cancer, blocking CD47-mediated SIRP $\alpha$  signaling with anti-CD47 mAbs induced phagocytosis of tumor cells by human and mouse macrophages (13–17).

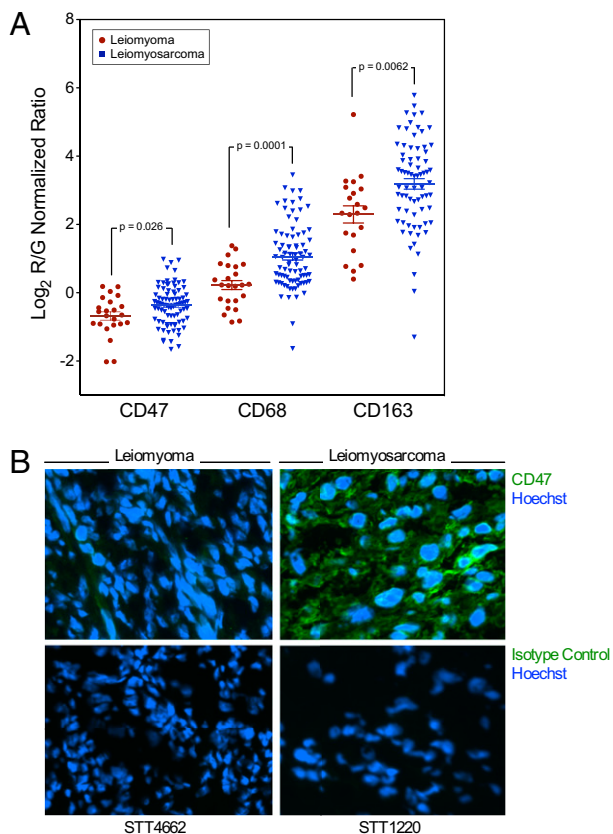


**Fig. 1.** Evaluation of CD47 expression in LMS versus benign leiomyoma. (A) Gene-expression profiling on 51 LMS and on 19 benign leiomyoma samples revealed that the transcript levels of *CD47*, as well as TAM markers *CD68* and *CD163*, were significantly higher on LMS versus their benign counterparts. *P* values were calculated using Student *t* test. (B) Immunofluorescence staining with anti-CD47 (Upper) or isotype control (Lower) antibodies on 16 LMS, three leiomyoma, and three normal muscle samples revealed that CD47 protein was more highly expressed on LMS than on benign or normal tissues. Representative images are shown and additional images are available Fig. S1 (see also Table S1). Magnification, 200 $\times$ .

Given the prognostic association of TAMs in LMS and the confirmation of CD47 expression in LMS patient samples, we developed an in vitro assay to study the interaction between LMS cells and macrophages with the hypothesis that anti-CD47 mAbs may enable phagocytosis of LMS cells by macrophages.

CD47 expression on human LMS cell lines LMS04 and LMS05 was confirmed using flow cytometry (Fig. 2A). Peripheral blood mononuclear cells (PBMCs) were purified from human whole blood and macrophages were enriched by plastic adherence for 1 wk. Nonadherent cells were removed and macrophage purity was confirmed using immunohistochemistry (IHC) for a panel of immune cell markers; PBMC-derived macrophages expressed CD68 and CD163 and only rare contaminating lymphocytes were seen, as evidenced by the absence of expression of CD3, CD4, CD8, and CD20 (Fig. 2B).

LMS04 and LMS05 were green fluorescently labeled and subsequently incubated with blocking (clone B6H12) or nonblocking (clone 2D3) anti-CD47 mAbs, or IgG control antibodies, before being cocultured with the PBMC-derived macrophages. B6H12-treated LMS04 and LMS05 cells were both readily phagocytosed by the human macrophages; in contrast, 2D3- or IgG-treated LMS04 and LMS05 cells were not phagocytosed by macrophages. Representative images of phagocytosis are shown for LMS05 in Fig. 2C.

To visualize this interaction in real time using live-cell imaging, red fluorescent protein (RFP)-positive macrophages were derived from the bone marrow of C57BL/*K<sub>a</sub>* Rosa26-mRFP1 mice and were incubated with green fluorescently labeled LMS05 cells, which had been treated with anti-CD47 (B6H12) or IgG antibodies. Consistent with the results observed with human macrophages, the red fluorescent mouse macrophages were able to efficiently phagocytose anti-CD47-treated cells, in contrast to IgG-treated cells, which were not phagocytosed by the macrophages (Fig. 3 and Movies S1, S2, and S3).

**Anti-CD47 Antibodies Inhibit Established Primary Tumor Growth.** We evaluated whether anti-CD47 mAbs could inhibit tumor growth of xenotransplanted LMS tumors in NOD/SCID/IL-2R $\gamma$ <sup>null</sup> (NSG) mice, which lack B, T, and NK cells but retain functional macrophages capable of phagocytosis (18). For the evaluation, 100,000 LMS04 or LMS05 cells were engrafted subcutaneously on the backs of NSG mice and, as soon as palpable tumors

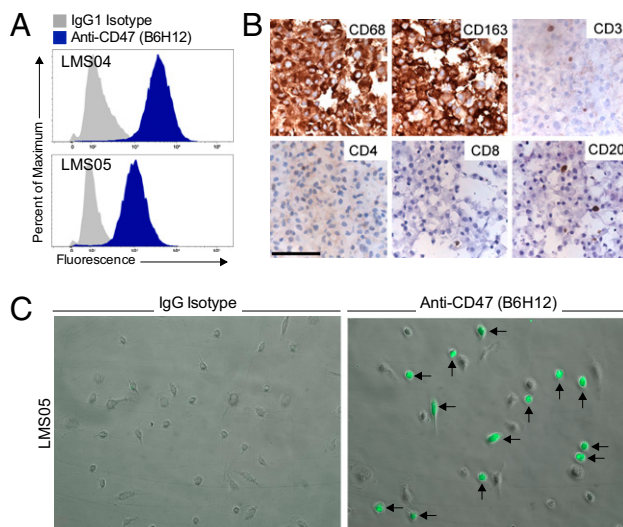


**Fig. 2.** In vitro system to study interaction between human macrophages and LMS cell lines. (A) CD47 protein expression was confirmed in human LMS cell lines, LMS04 and LMS05, by flow cytometry. (B) PBMC-derived macrophages were assessed by IHC for a panel of immune markers. Scale bar, 50  $\mu$ m. (C) Representative images showing that anti-CD47 mAb treatment resulted in robust phagocytosis of green fluorescently labeled LMS05 cells by human macrophages (arrows), whereas treatment of LMS05 cells with control antibodies resulted in no phagocytosis. Magnification, 200 $\times$ .



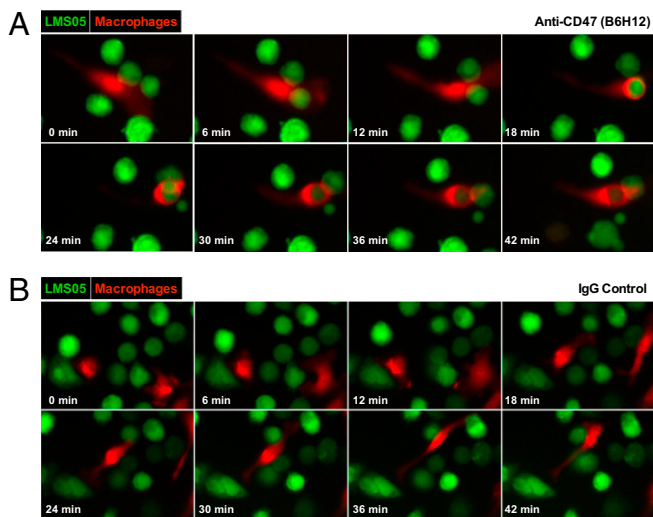


**Fig. 3.** Real-time monitoring of LMS cell phagocytosis by macrophages. RFP-positive mouse macrophages (red) and fluorescently labeled LMS05 cells (green) were cocultured in the presence of anti-CD47 (A) or IgG (B) antibodies and were imaged using video microscopy. (Movies S1, S2, and S3).

appeared (2 wk), mice were treated with a fully humanized anti-CD47 mAb (clone B6H12) or human IgG by intraperitoneal injections three times per week (full details of treatment protocol are in Table S2). At the conclusion of the experiment, animals were killed and tumor presence was confirmed by H&E staining and Vimentin IHC. We found that treatment with anti-CD47 mAbs dramatically inhibited tumor growth of both LMS04 and LMS05 xenotransplanted tumors, with LMS05 showing a greater than fivefold decrease in average tumor mass ( $t$  test,  $P = 0.0001$ ) and LMS04 showing a greater than 30-fold decrease in average tumor mass ( $t$  test,  $P = 0.0188$ ) (Fig. 4 A–D).

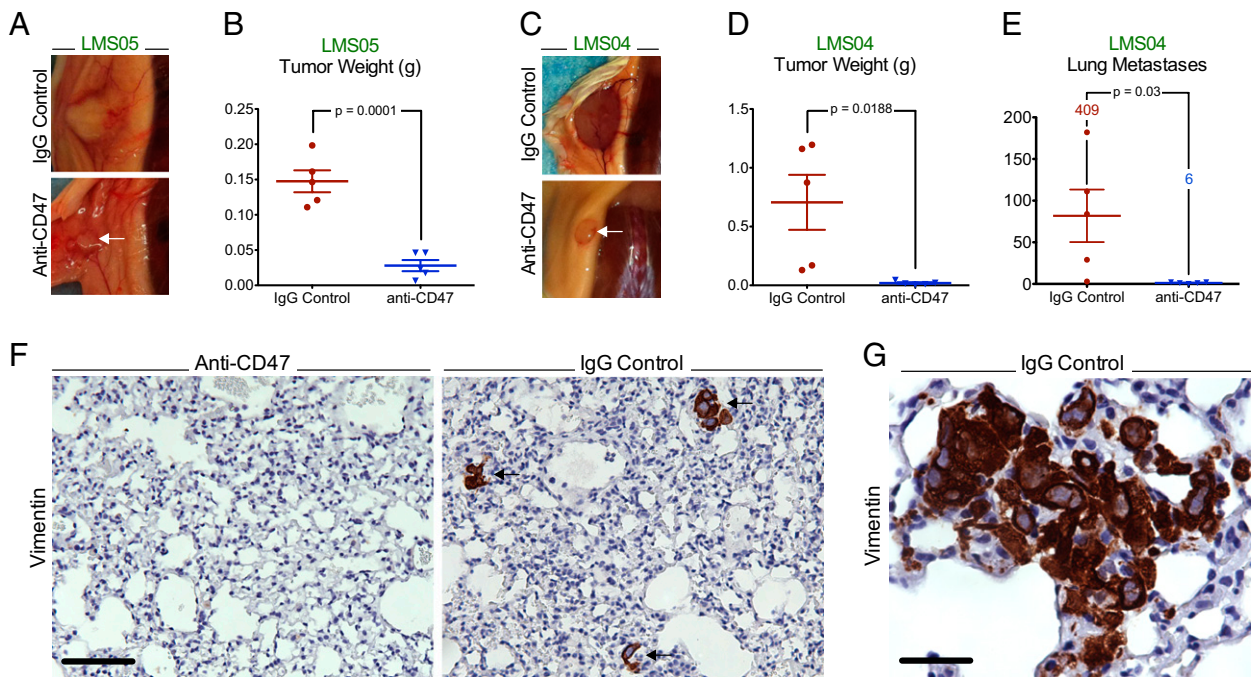


**Fig. 4.** Effect of anti-CD47 treatment on primary tumor growth in xenotransplantation models of LMS. Representative tumors (A) and comparison of primary tumor volumes (B) of LMS05 xenografts treated with anti-CD47 or IgG antibodies. Representative tumors (C), comparison of primary tumor volumes (D), and comparison of the presence of lung metastases (E) of LMS04 xenografts treated with anti-CD47 or IgG antibodies.  $P$  values were calculated using Student  $t$  test. (F) Vimentin IHC on representative lungs from anti-CD47 or IgG control-treated mice. Scale bar, 40  $\mu$ m. (G) Example of multicell metastatic focus from IgG control-treated mouse lung. Scale bar, 25  $\mu$ m.

Histological analysis of LMS04- and LMS05-engrafted mice was performed to evaluate the presence of distant metastases. In LMS05-engrafted mice, lungs, livers, kidneys, spleens, hearts, and brains showed no evidence of metastatic disease, as evaluated by H&E staining and Vimentin IHC. In contrast, metastases developed in the lungs of LMS04-engrafted mice. In the IgG control-treated mice, a total of 409 lung metastases were observed in the five mice, whereas only six metastatic growths were observed in the lungs of the five mice receiving anti-CD47 mAbs, representing a nearly 70-fold decrease in the metastatic potential of LMS04 xenotransplanted tumors upon anti-CD47 mAb treatment ( $t$  test,  $P = 0.03$ ) (Fig. 4E). Notably, the six pulmonary metastases observed in the anti-CD47 mAb-treated mice were all single-cell growths, whereas IgG-control-treated mice showed significant numbers of well-established multicell metastatic clusters (Fig. 4F and G).

**Development of a Metastatic Model of LMS.** Distant metastases and tumor recurrences after primary tumor resections are the principal factors underlying mortality in LMS patients and represent significant challenges to the clinical management of these tumors (2, 3). We therefore sought to recapitulate the progression of the human disease by developing a metastatic xenotransplantation model of LMS. One hundred thousand LMS04 cells were engrafted subcutaneously on the backs of 14 NSG mice and individual animals were killed each week to check for the presence of lung metastases (Fig. 5A). At early time points, mice showed no evidence of lung metastases, indicating that the metastatic growths observed at later time points in the IgG-treated LMS04-engrafted mice were not resulting from the initial tumor injection procedure, but rather were originating from the primary tumors (Fig. 5B). Six weeks after subcutaneous injection of tumor cells on the back, LMS04 tumor cells started to appear as single cells in the lungs, as determined by H&E staining and Vimentin IHC. At this time the primary tumors in the remaining eight mice were resected and individual mice were killed each week to assess the progression of the metastatic lung growths. Postresection, the number and size of metastases in the lungs increased over time (Fig. 5B) and mice also developed secondary axillary lymph-node

tumors, which were confirmed as originating from the LMS04 cells by H&E analysis and by Vimentin IHC (Fig. 5C).

**Anti-CD47 Antibodies Are Effective in a Model for Neoadjuvant Therapy.** We tested whether anti-CD47 mAb treatment could show efficacy in a model for neoadjuvant therapy using the metastatic xenotransplantation model of LMS04: 100,000 LMS04 cells were transplanted subcutaneously on the backs of NSG mice and were allowed to grow for 6 wk, the time point that we previously determined to correspond to the onset of lung metastases. Mice were then randomized based on tumor size, treated for 1 wk with anti-CD47 mAb or IgG control antibodies, and the primary tumors were surgically resected (Fig. 6A and Table S3). After resection, the antibody treatments continued; the mice were monitored daily and the presence of metastatic tumor deposits in the axillary region was recorded. All primary tumor grafts that grew on the backs of mice were lateral to the spine and metastatic deposits always occurred in the axillary area on the same side of the mouse. We therefore interpret these deposits as lymphatic metastases to axillary lymph nodes. Anti-CD47 mAb treatment increased recurrence-free survival after primary tumor resections, as measured by time to presence of axillary lymph-node tumors (Fig. S2). In addition to delaying the onset of these lymph-node tumors, anti-CD47 mAb treatment led to a nearly threefold decrease in average volume of the lymph-node tumors (*t* test, *P* = 0.05) and diminished the total number of lymph-node tumors observed. IgG treatment resulted in a total of 10 lymph-node tumors distributed over six mice and anti-CD47 mAb treatment resulting in a total of five lymph-node tumors distributed over six mice (Fig. 6B and C).

Importantly, anti-CD47 mAb treatment almost completely inhibited the formation of lung metastases after resection of the primary tumor grafts. A computational morphometric approach was used to quantify the number of Vimentin-positive stained cells in whole sections of mouse lungs. Five control mice that did not carry LMS04 xenografts were used to determine the background staining

and the six mice from each group (IgG or anti-CD47-treated) were scored. The results are shown in Table S4 and show a significant difference between the two groups. Histologic examination of the lung sections confirmed the quantitative measurement and, furthermore, showed that two types of metastatic deposits could be identified: those consisting of single cells and those that contained two or more cells in a tight cluster. Single-cell metastatic deposits were found in all 12 mice, whereas multicell metastatic clusters were found almost exclusively in the IgG control group. Two anti-CD47-treated mice (#650 and #550) showed an exception to this rule and had four and one multicell foci containing more than four cells, respectively; these foci were small (< 10 cells) and were associated with inflammatory cells and fibrin depositions, morphologic features that suggest degradation of the cells in the metastatic growths. (Fig. 6F). One of the six anti-CD47-treated mice (#540) did not show a single metastatic cell in the whole-lung sections, and the remaining five mice had scattered single cells throughout the lung parenchyma, explaining the variable degree of Vimentin reactivity measured in Table S4. Fig. 6G further illustrates the differences in lung metastases between the two groups, showing that the anti-CD47-treated mouse with the highest lung metastasis score (#548) had only scattered individual cells in the lungs, whereas the IgG control mouse with the lowest score (#2798) had four foci of multicell clusters. Together, these results indicate that anti-CD47 mAbs may be effective as neoadjuvant therapeutic treatment options with the potential to address the significant clinical problem of distant metastases after primary LMS tumor resection.

### Discussion

Macrophages can exert distinct functions, such as the classically activated (M1) pathway that is involved in the response of type I helper T cells to pathogens and that includes the ability to phagocytose, and the alternatively activated (M2) pathway that is involved in type II helper T-cell processes in wound healing and humoral immunity. Other macrophage activation pathways, the classifications of which are less clear, also exist and play roles in developmental processes and tissue repair. In cancer, it is thought that M1 macrophages are able to inhibit tumor growth, whereas M2 macrophages generally promote neoplasia and tumor progression. In most cancers, such as breast, thyroid, lung, and hepatocellular carcinomas, macrophage presence correlates with poor patient outcome, suggesting that the M2 phenotype predominates. However, in other cancers, such as pancreatic cancer, TAMs are indicative of a less-aggressive tumor, consistent with the notion that macrophages possess the capacity to inhibit or potentiate tumor growth, depending on their polarization (4–6).

The TME has been studied in most detail in epithelial neoplasms, possibly because in carcinomas the demarcation between tumor cells and their microenvironment is readily recognizable upon histological evaluation. In sarcomas, relatively little study has been performed on the TME. We initially began our investigation of the TME in sarcomas using gene-expression profiling and found that in LMS, but not in most other sarcoma types, individual cases could have significantly increased TAMs. We further investigated this finding using IHC and *in situ* hybridization studies on tissue microarrays with associated patient outcome data, and found that the presence of TAMs correlated with poor patient outcome. TAM infiltration was likely mediated by expression of CSF1 by the tumor cells. In nongynecological LMS, the presence of TAMs was associated with increased vessel density, suggesting that the poor clinical outcome seen in these tumors could in part be because of increased vascularity mediated by TAMs (7–9). Hence, the M2 phenotype likely predominates in TAMs present in LMS tumors as it does in most, but not all, epithelial tumors.

Inhibition of CD47 using monoclonal antibodies has been shown to effectively allow phagocytosis of cancer cells by macrophages in experimental models of leukemia, lymphoma, and carcinomas (13–17). However, the relevance of this molecule in sarcomas has yet to be studied. In the present study, we show that inhibiting the antiphagocytic function of CD47 allows for both human and mouse macrophages to phagocytose LMS cells *in vitro*. Furthermore, in two xenotransplantation models of LMS, we are unique in showing that treatment with fully humanized

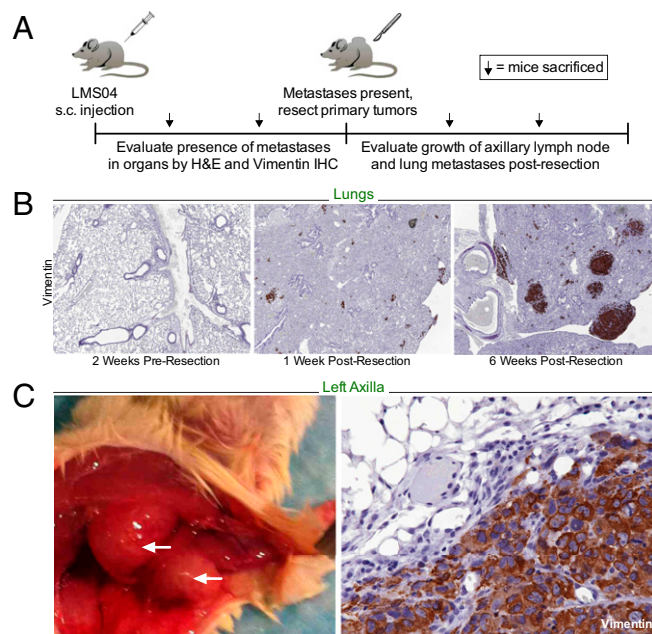


**Fig. 5.** Characterization of metastatic model of LMS. (A) Mice were injected subcutaneously with 100,000 LMS04 cells and individual mice were killed at weekly intervals until the appearance of single-cell lung metastases. Thereafter, primary tumors were resected and the remaining mice were serially killed to assess the progression of lung metastases and secondary tumor outgrowth in the axilla. (B) Representative Vimentin IHC stains on mouse lungs 2 wk before primary tumor resection, 1 wk after primary tumor resection, and 6 wk after primary tumor resection. Magnification, 40 $\times$ . (C) Autopsy image (Left) and Vimentin IHC (Right) of axillary region of mouse that had developed two lymph-node tumors after resection of primary tumor.



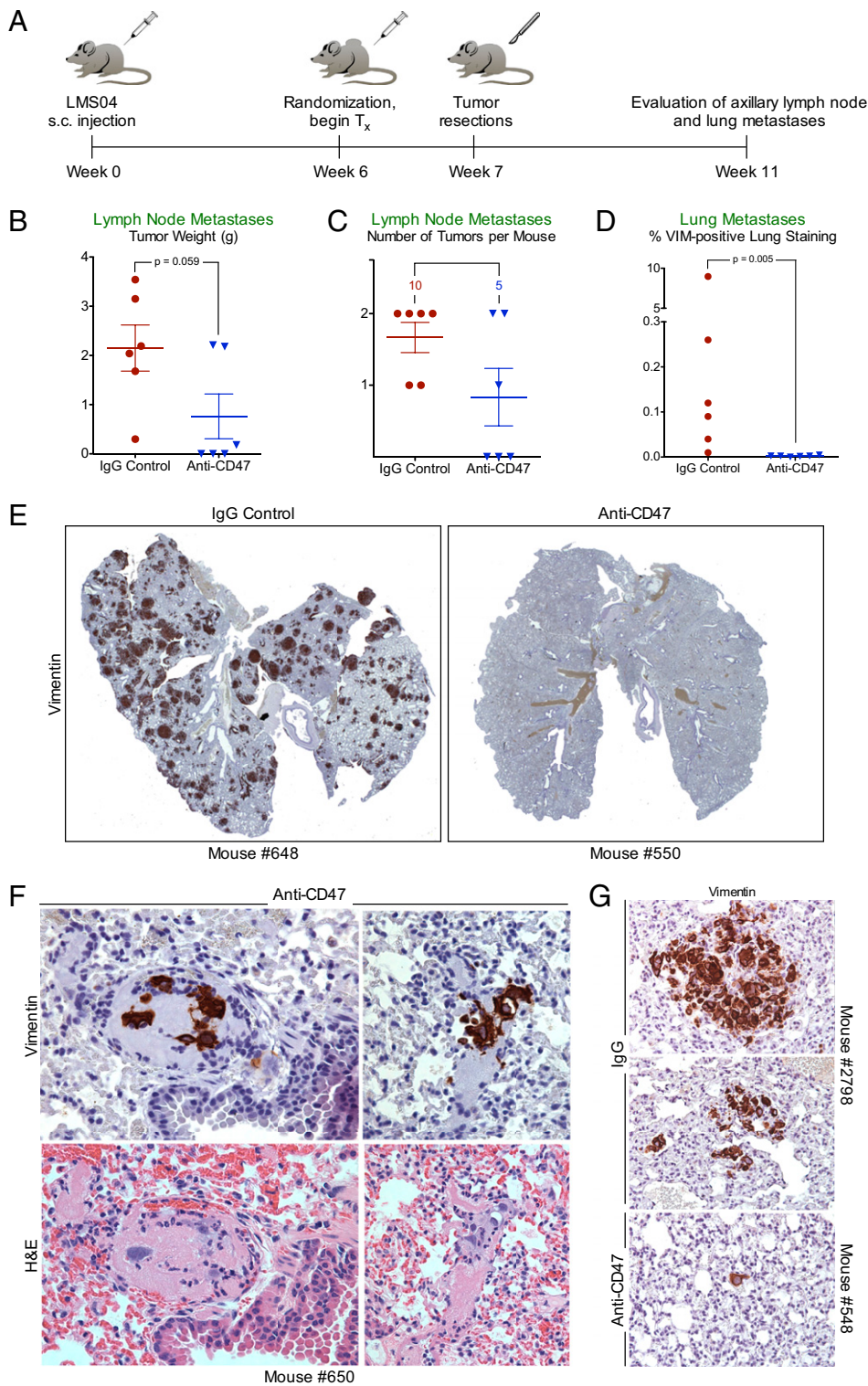


**Fig. 6.** Effect of anti-CD47 therapy in neoadjuvant treatment model. (A) Mice were implanted subcutaneously with 100,000 LMS04 cells. Tumor volumes were measured at week 6, and mice with a similar range of tumor sizes were assigned to either anti-CD47 or IgG treatment groups (as detailed in Table S3). Effect of anti-CD47 antibody treatment on the volume (B) and incidence (C) of secondary lymph-node tumors. *P* values were calculated using Student *t* test. (D) Effect of anti-CD47 antibody treatment on the presence of lung metastases, as measured using computerized morphometric analysis. *P* value calculated using Wilcoxon rank-sum test. (E) Sample lungs from IgG control-treated or anti-CD47-treated lungs. (F) Presence of fibrin deposits, inflammatory cells, and degraded tumor cells in lung metastases of mouse treated with anti-CD47 antibodies. Magnification, 400 $\times$ . (G) Comparison of multicell clusters and single-cell growths in IgG control or anti-CD47-treated mouse lungs. Magnification, 200 $\times$ .

anti-CD47 monoclonal antibodies inhibits primary tumor growth, thereby suggesting that anti-CD47 therapy may be an effective means of treating primary LMS tumors. We noted that in one of the xenotransplanted cell lines (LMS04) pulmonary metastases resulted, which decreased in size and number upon treatment with anti-CD47 mAbs. Although the primary effect of anti-CD47 is likely to be via the TAMs, other hemolymphoid cells express SIRP $\alpha$ , and in this article we have not analyzed whether multiple effectors could be involved. Furthermore, although T-cells have

also been shown to potentially mediate TAM polarization, this mechanism was not investigated in the present work, as the NSG mice used for our *in vivo* experiments lack functional T-cells (5).

In most human LMS cases, the initial tumor can be surgically resected and radiation therapy is often an effective approach for inhibiting the recurrence of the primary tumor. Although the primary tumor growth can often be controlled, a significant fraction of LMS tumor lethality is because of metastatic disease (1–3). Here, we developed a xenotransplantation model of

metastatic LMS, whereby tumor cells were injected subcutaneously on the backs of mice and were allowed to grow without intervention until they became large and well established. Upon resection of these primary tumors, metastatic tumors appeared in both the ipsilateral axillary lymph node and the lungs of all mice. At early time points, no tumor cells were present in the lungs, as evidenced by histological examination and staining of whole-lung sections for Vimentin, indicating that the presence of metastases at later time points represents true metastatic disease rather than the seeding of tumor cells into the bloodstream of lymphatic vasculature at the time of the subcutaneous xenotransplantation of the tumor cells. Starting at week 6, small single-cell metastases were found in the lungs, and these clusters grew in size and number over time.

In an effort to mimic neoadjuvant therapy in human LMS patients, we allowed primary tumors to become established and started anti-CD47 therapy 1 wk before resection of the primary tumors at 7 wk. In this system, which allowed us to specifically study the effect of therapeutic intervention on the progression of metastatic disease, we found that anti-CD47 therapy diminished the size and incidence of axillary lymph-node tumor growth and almost completely inhibited the formation of lung metastases. These results suggest that anti-CD47 therapy may effectively diminish metastatic disease burden in LMS, which poses a significant challenge in the clinical management and survival of patients with these tumors. In addition to established, multicell metastases that were present in the IgG-treated (and to a much lesser extent, in the anti-CD47-treated) lungs, single-cell metastases were seen in both groups. It is possible that, rather than representing viable metastases, these single cells may instead represent arrested tumor cells that are known to lead to actual metastases in only 1–5% of instances (19, 20). Moreover, in the group of six mice treated with anti-CD47 mAb, a total of only eight foci of metastases consisting of two to nine cells each were found. Several of these foci were associated with a dense inflammatory infiltrate and showed histologic features suggesting tumor cell degradation.

In conclusion, we have found that CD47 is expressed on LMS tumor cells and we have demonstrated that inhibiting CD47 function using monoclonal antibodies is an effective method of treating LMS tumors in vitro and in vivo, thereby forming the rationale for evaluating the clinical efficacy of anti-CD47 therapy in human patients with LMS tumors. Further studies are needed to address the relationship between the density of TAMs and the efficacy of anti-CD47 treatment in LMS, and subsequently to explore the possibility of combining anti-CD47 mAb therapy with treatments that modulate the CSF1 pathway in order harness TAMs as biological tools to decrease tumor growth in patients with LMS.

## Materials and Methods

**Case Selection and Gene-Expression Profiling.** The clinicopathologic features of the 51 LMS tumor samples and of the 19 leiomyoma samples used in this study

have been described previously (21). Gene-expression profiling was performed using 44 K spotted cDNA microarrays and expression values of CD47, CD68, and CD163 were compared between LMS and leiomyoma samples using Student *t* tests. Gene-expression data can be accessed from the Stanford Microarray Database (<http://smd.stanford.edu>) (22). Gene-expression studies were performed with the approval of the Stanford University Institutional Review Board.

**Immunohistochemistry.** CD47 protein expression was evaluated by fluorescent IHC on OCT-embedded, fresh-frozen tissue, as described in *SI Materials and Methods*. Colorimetric IHC on formalin-fixed, paraffin-embedded cell pellets from PBMC-derived human macrophages and on full cross-sections of formalin-fixed, paraffin-embedded mouse organs are also described in *SI Materials and Methods*.

**Cell Culture.** LMS04 and LMS05 cells were cultured as described in *SI Materials and Methods*.

**Flow Cytometry.** LMS04 and LMS05 cell suspensions were stained with phycoerythrin-conjugated anti-CD47 (BD PharmMingen) or isotype control antibodies. CD47 expression was analyzed by flow cytometry on a BD FACSAria instrument (Becton Dickinson).

**In Vitro Phagocytosis Assays.** Human macrophages were prepared from PBMCs, as described previously (14), and in vitro phagocytosis assays were performed as described in *SI Materials and Methods*.

**Live-Cell Imaging of Macrophage Phagocytosis in Vitro.** RFP-positive mouse macrophages were prepared from C57BL/K<sub>a</sub> Rosa26-mRFP1 transgenic mice (23) and live-cell imaging of macrophage phagocytosis was performed as described in *SI Materials and Methods*.

**Xenotransplantation Experiments.** Primary tumor growth experiments and treatment protocols are described in *SI Materials and Methods* and *Table S2*. The development of the metastatic tumor model, and experiments evaluating the effects anti-CD47 treatment on metastatic disease, are described in *SI Materials and Methods* and *Table S3*. All procedures followed protocols approved by the Stanford Committee on Animal Research.

**Morphometrics Analysis.** To assess metastatic tumor presence in the lungs, we performed IHC for human Vimentin, which does not react with murine tissue, and then performed morphometric analyses as described in *SI Materials and Methods*.

**ACKNOWLEDGMENTS.** We thank Roger Warnke, Norm Cyr, Alayne Brunner, Kelli Montgomery, Shirley Zhu, and members of the Stanford Immunodiagnosis Laboratory for helpful discussions and assistance with experimental design and optimization. B.E. is a recipient of the National Science Foundation Graduate Research Fellowship. This work was supported by National Institutes of Health Grant CA 112270 and grants from the National Leiomyosarcoma Foundation, the LMSarcoma Direct Research Foundation, and the Ludwig Institute for Cancer Research.

- Evans HL, Shipley J (2002) *Pathology and Genetics of Tumours of Soft Tissue and Bone—World Health Organization Classification of Tumours*, eds Fletcher CDM, Unni KK, Mertens F (IARC Press, Lyon), pp 131–134.
- Coindre JM, et al. (2001) Predictive value of grade for metastasis development in the main histologic types of adult soft tissue sarcomas: A study of 1240 patients from the French Federation of Cancer Centers Sarcoma Group. *Cancer* 91:1914–1926.
- Blay JY, et al. (2003) Advanced soft-tissue sarcoma: A disease that is potentially curable for a subset of patients treated with chemotherapy. *Eur J Cancer* 39:64–69.
- Lewis CE, Pollard JW (2006) Distinct role of macrophages in different tumor micro-environments. *Cancer Res* 66:605–612.
- Qian BZ, Pollard JW (2010) Macrophage diversity enhances tumor progression and metastasis. *Cell* 141:39–51.
- Jaiswal S, Chao MP, Majeti R, Weissman IL (2010) Macrophages as mediators of tumor immunosurveillance. *Trends Immunol* 31:212–219.
- Lee CH, et al. (2008) Prognostic significance of macrophage infiltration in leiomyosarcomas. *Clin Cancer Res* 14:1423–1430.
- Espinosa I, et al. (2009) Coordinate expression of colony-stimulating factor-1 and colony-stimulating factor-1-related proteins is associated with poor prognosis in gynecological and nongynecological leiomyosarcoma. *Am J Pathol* 174:2347–2356.
- Espinosa I, et al. (2011) CSF1 expression in nongynecological leiomyosarcoma is associated with increased tumor angiogenesis. *Am J Pathol* 179:2100–2107.
- Kubota Y, et al. (2009) M-CSF inhibition selectively targets pathological angiogenesis and lymphangiogenesis. *J Exp Med* 206:1089–1102.
- Brown EJ, Frazier WA (2001) Integrin-associated protein (CD47) and its ligands. *Trends Cell Biol* 11:130–135.
- Barclay AN, Brown MH (2006) The SIRP family of receptors and immune regulation. *Nat Rev Immunol* 6:457–464.
- Jaiswal S, et al. (2009) CD47 is upregulated on circulating hematopoietic stem cells and leukemia cells to avoid phagocytosis. *Cell* 138:271–285.
- Majeti R, et al. (2009) CD47 is an adverse prognostic factor and therapeutic antibody target on human acute myeloid leukemia stem cells. *Cell* 138:286–299.
- Chao MP, et al. (2010) Anti-CD47 antibody synergizes with rituximab to promote phagocytosis and eradicate non-Hodgkin lymphoma. *Cell* 142:699–713.
- Chao MP, et al. (2010) Calreticulin is the dominant pro-phagocytic signal on multiple human cancers and is counterbalanced by CD47. *Sci Transl Med* 2:63ra94.
- Chao MP, et al. (2011) Therapeutic antibody targeting of CD47 eliminates human acute lymphoblastic leukemia. *Cancer Res* 71:1374–1384.
- Ito M, et al. (2002) NOD/SCID/gamma(c)(null) mouse: An excellent recipient mouse model for engraftment of human cells. *Blood* 100:3175–3182.
- Cameron MD, et al. (2000) Temporal progression of metastasis in lung: Cell survival, dormancy, and location dependence of metastatic inefficiency. *Cancer Res* 60:2541–2546.
- Chen Q, Zhang XH, Massagué J (2011) Macrophage binding to receptor VCAM-1 transmits survival signals in breast cancer cells that invade the lungs. *Cancer Cell* 20:538–549.
- Beck AH, et al. (2010) Discovery of molecular subtypes in leiomyosarcoma through integrative molecular profiling. *Oncogene* 29:845–854.
- Sherlock G, et al. (2001) The Stanford Microarray Database. *Nucleic Acids Res* 29:152–155.
- Ueno H, Weissman IL (2006) Clonal analysis of mouse development reveals a polyclonal origin for yolk sac blood islands. *Dev Cell* 11:519–533.